Lithium Ion Dynamics in $LiZr_2(PO_4)_3$ and $Li_{1.4}Ca_{0.2}Zr_{1.8}(PO_4)_3$

Isabel Hanghofer,[1,*] Bernhard Gadermaier,[1] Alexandra Wilkening,[1] Daniel Rettenwander[1] and H. Martin R. Wilkening[1,2,†]

[1] *Institute for Chemistry and Technology of Materials, Christian Doppler Laboratory for Lithium Batteries, Graz University of Technology (NAWI Graz), Stremayrgasse 9, A-8010 Graz, Austria*

[2] *ALISTORE – European Research Institute, CNRS FR3104, Hub de l'Energie, Rue Baudelocque, 80039 Amiens, France*

* *corresponding author, e-mail: isabel.hanghofer@tugraz.at*

† *see also for correspondence, e-mail: wilkening@tugraz.at*

Figure **S1a** shows the X-ray powder diffraction pattern of $LiZr_2(PO_4)_3$ as it is obtained after the calcination step carried out at 900 °C but before sintering at 1150 °C in a Al_2O_3 crucible. The crystal structure of the monoclinic phase is also depicted. In Figure **S1b** the change in ionic conductivity is shown before and after the sintering procedure. While the total ionic conductivity, including the influence of grain boundaries, is thermally activated by 0.83 eV, after sintering, *i.e.*, in rhombohedral LZP, the activation energy E_a reduces to 0.37 eV (*cf.* temperatures above ambient). This decrease in E_a is accompanied by a clear increase in ionic conductivity. Open symbols in Figure **S1b** represent bulk ionic conductivities as obtained from analysing conductivity isotherms, see Figure 4. As for the rhombohedral sample, the isotherms are composed of two plateaus referring to i) ionic conductivities affected by g.b. and ii) regions solely reflecting the electrical response of the bulk.

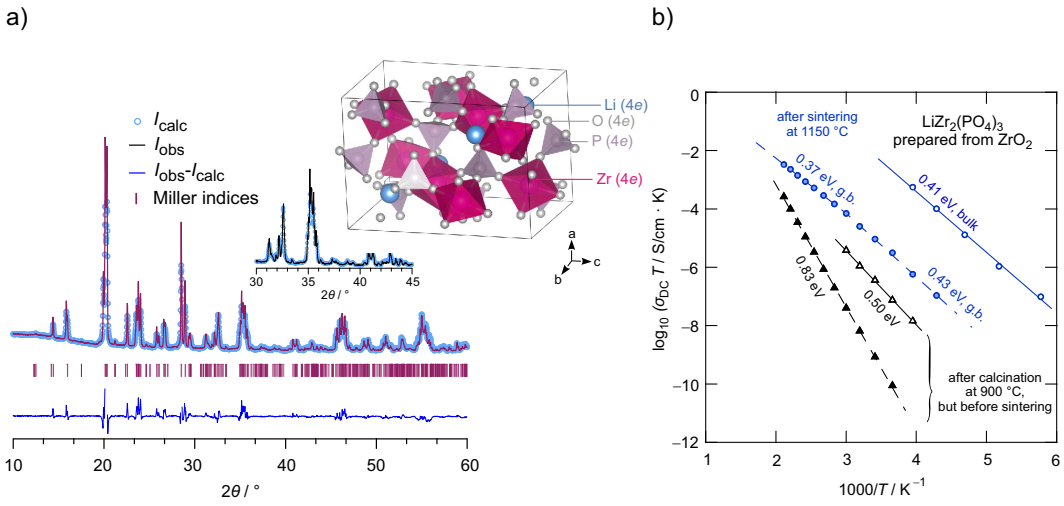

Figure S1: a) X-ray powder diffraction pattern of $LiZr_2(PO_4)_3$ (LZP) prepared from ZrO_2 at 900 °C. LZP crystallizes with monoclinic symmetry (space group $P12_1/c1$). Selected reflections have been indexed with vertical bars. An almost negligible amount of ZrO_2 can be seen, the amount corresponds to only 2.0 wt. %. Inset: Illustration of the monoclinic structure of LZP. Blue spheres represent Li^+ cations; ZrO_6 octahedra and PO_4 tetrahedra are shown in pink and violet colours, respectively. Grey spheres show oxygen anions. b) Change of $\log_{10}(\sigma_{DC}T)$ as a function of the inverse temperature $1000/T$ of LZP before and after sintering. While filled symbols represent ionic conductivities including the resistive g.b. regions, open symbols characterise the response of the bulk regions.

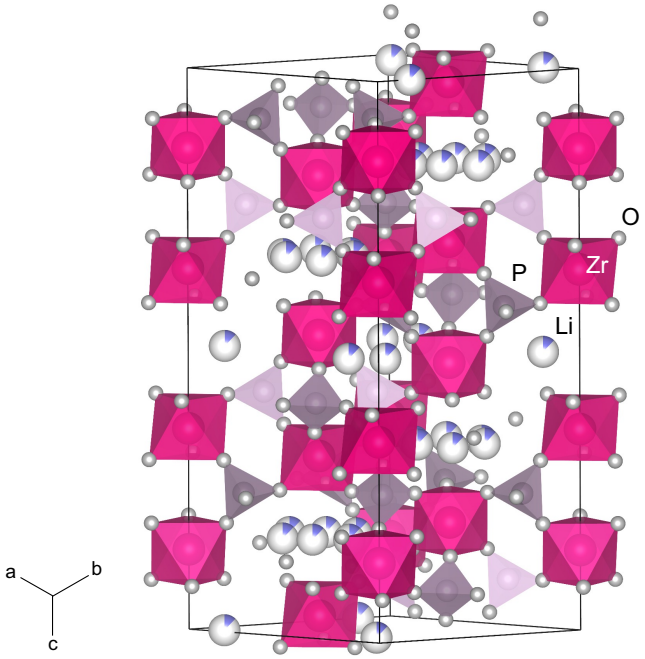

Figure S2: Structure of α-$LiZr_2(PO_4)_3$ as obtained by high-temperature neutron diffraction carried out by Catti *et al.* (see M. Catti, A. Comotti and S. Di Blas, *Chem. Mater.*, 2003, **15**, 1628-1632).

Table S1: Lattice and fitting parameters as obtained from X-powder diffraction structure solution pointing to *R*-3*c* symmetry after the sintering process. LCZP0.1 and LCZP0.2 refer to either $Li_{1.2}Ca_{0.1}Zr_{1.9}(PO_4)_3$ and $Li_{1.4}Ca_{0.2}Zr_{1.8}(PO_4)_3$. With increasing Ca-content we see that the lattice parameters change indicating Ca^{2+} incorporation into the structure. GoF means goodness of fit (GoF); the weighted R-profile (R_{wp}) and the R-Bragg values (R_{exp}) are also included.

	Lattice Parameters			**Fitting parameters**		
Sample	***a* / Å**	***c* / Å**	***V* / Å³**	R_{wp}	R_{exp}	**GoF**
LZP (from ZrO_2)	8.824	22.456	1514.24	9.96	4.19	5.64
LZP (from $Zr(ac)_4$)	8.819	22.477	1513.99	15.60	5.59	7.77
LCZP0.1 (ZrO_2)	8.842	22.341	1512.64	11.94	4.59	6.75
LCZP0.2 (ZrO_2)	8.854	22.186	1506.22	10.48	5.23	4.01

Figure **S3** shows the Nyquist plots of $LiZr_2(PO_4)_3$ and $Li_{1.4}Ca_{0.2}Zr_{1.8}(PO_4)_3$ recorded at 213 K. We used suitable equivalent circuits to estimate the capacities of the depressed semicircles shown. Both samples show typical values for bulk and grain boundary processes, these are in agreement with those estimated from both permittivity spectra and the modulus representation.

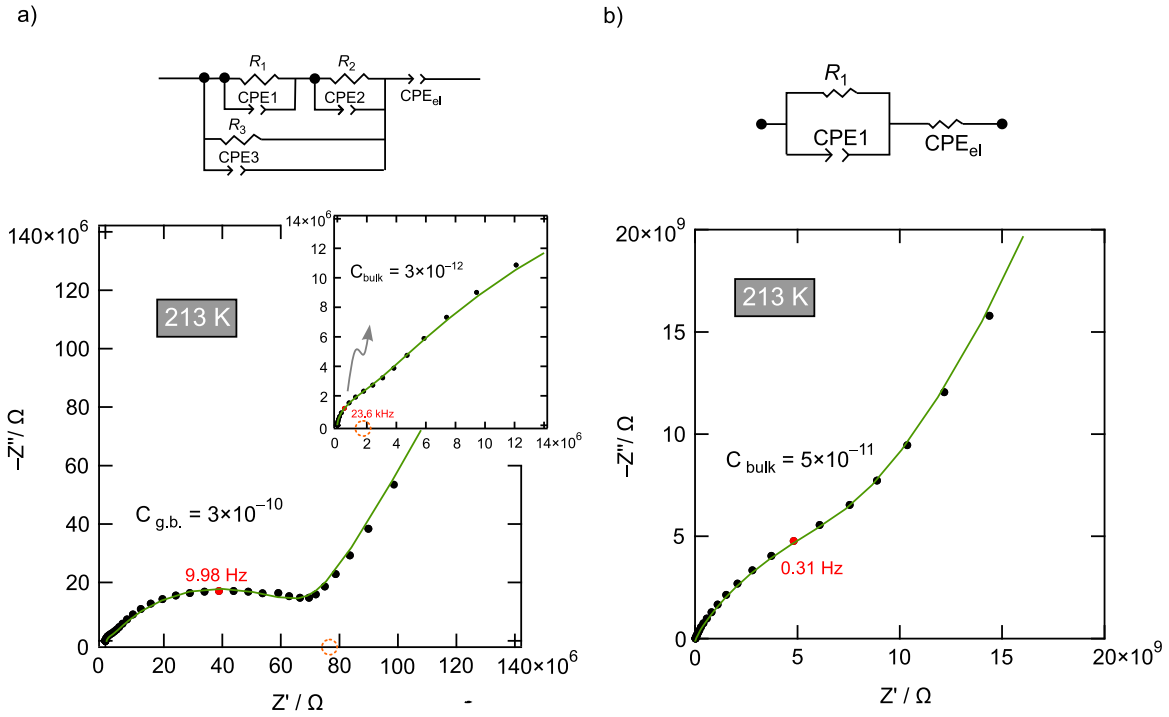

Figure S3: Nyquist representation of the complex impedance data (real part Z′ vs. the imaginary part Z″) of a) $Li_{1.4}Ca_{0.2}Zr_{1.8}(PO_4)_3$ and b) $LiZr_2(PO_4)_3$ at 213 K. In a) two depressed semicircles are seen reflecting the bulk (high frequency region) and the grain boundary response (low frequency range). This separation turned out to be very difficult for $LiZr_2(PO_4)_3$ as the two responses merge into each other. The equivalent circuits used to analyse the data are shown at the top (CPE: constant phase element; R_i: resistance, i = 1, 2, 3).